

Calculations of the hurricane eye motion based on singularity propagation theory *

Vladimir Danilov, Georgii Omel'yanov, & Daniil Rozenknop

Abstract

We discuss the possibility of using calculating singularities to forecast the dynamics of hurricanes. Our basic model is the shallow-water system. By treating the hurricane eye as a vortex type singularity and truncating the corresponding sequence of Hugoniot type conditions, we carry out many numerical experiments. The comparison of our results with the tracks of three actual hurricanes shows that our approach is rather fruitful.

1 Introduction

In this paper we discuss a possibility of using an approach related to calculating singularities for numerical modeling the dynamics of hurricanes.

It is well known that for a detailed mathematical description of large-scale and meso-scale processes in the atmosphere one needs to use very complicated systems of nonlinear partial differential equations based on equations of three-dimensional gas dynamics (e.g., see [1–5]). So far it is impossible to solve such systems numerically in real time, therefore, one must use different simplifying assumptions. The first simplification is to neglect viscosity and heat conduction effects. As a result, the order of equations decreases and the problem of posing boundary conditions disappears. Further possible simplifications (neglect of vertical displacements, heat exchange effects, etc.) lead to comparatively simple models, the simplest of which is the so-called shallow-water system

$$\begin{aligned}\frac{\partial U}{\partial t} + \langle U, \nabla \rangle U + \nabla z &= f\Pi U, \\ \frac{\partial z}{\partial t} + \langle \nabla, zU \rangle &= 0.\end{aligned}\tag{1}$$

Here $U = (u, v)$ is the vector of horizontal velocity, Π is the matrix of rotation through $\pi/2$ ($\Pi_{11} = \Pi_{22} = 0$, $\Pi_{12} = -\Pi_{21} = 1$), f is the Coriolis parameter, and z is the geopotential.

* *Mathematics Subject Classifications:* 35D99, 86A10.

Key words: asymptotic behavior, forecast, hurricane.

©2002 Southwest Texas State University.

Submitted November 7, 2001. Published February 18, 2002.

At the same time, if we neglect dissipative effects, then the solution loses its smoothness. The fact that the solution is singular, allows us to calculate its dynamics by using rather powerful tools developed within the framework of the theory of generalized functions. Roughly speaking, these tools allow us to avoid finding the solution in the entire range of variables and thus only to determine the dynamics of the singularity support. Besides of a natural simplification due a decrease in the dimension of the problem, this approach allows us to avoid a very difficult problem of choosing the initial data in the entire range of spatial variables. Namely, existing monitoring facilities do not allow one to determine the initial distributions of velocity, density, and temperature with sufficient accuracy for large-scale formations. Simultaneously, the hurricane trajectory (the singularity support) can be fixed well by satellite imaging.

V. P. Maslov [6] proposed the hypothesis that a solution with a weak singularity whose singular support is of codimension 2 corresponds to the center of a hurricane. Such solution admits the representation

$$U = U^0(x, t) + \sqrt{S(x, t)}U^1(x, t), \quad z = z^0(x, t) + \sqrt{S(x, t)}z^1(x, t), \quad (2)$$

where U^i , z^i and S are smooth functions and

$$S \geq 0, \quad \nabla S \Big|_{S=0} = 0, \quad \text{Hess } S \Big|_{S=0} > 0. \quad (3)$$

To find the trajectory $\Gamma = \{(x, t), S(x, t) = 0\}$ of the singularity support, i.e., of a moving point, we substitute a solution of the form (2) into the equation (e.g., into (1)), which leads to the relation

$$D^0 + S^{-1/2}D^1 = 0, \quad (4)$$

where D^i are smooth functions. In turn, (4) implies the relations

$$\frac{\partial^{|\alpha|}}{\partial x^\alpha} D^i \Big|_{\Gamma} = 0, \quad |\alpha| = 0, 1, \dots, \quad i = 0, 1, \quad (5)$$

which lead to necessary conditions for the existence of a solution of the form (2). Maslov called these conditions *Hugoniot type conditions* (by analogy with the Hugoniot condition for shock waves). The above scheme was realized by Maslov and Zhikharev [6, 7] for the shallow-water system without Coriolis effects and by group of authors [8] for the system (1) with the Coriolis force. Hugoniot type conditions form an infinite non-triangular system. The first 14 equations of them have the form [8]

$$\begin{aligned} \dot{z}_0^0 &= -2qz_0^0, \\ \dot{V}_1 &= fV_2 - z_{10}^0, \\ \dot{V}_2 &= -fV_1 - z_{01}^0, \\ \dot{z}_{10}^0 &= -3qz_{10}^0 + pz_{01}^0 - z_0^0(v_{11}^0 + 2u_{20}^0), \\ \dot{z}_{01}^0 &= -3qz_{01}^0 - pz_{10}^0 - z_0^0(u_{11}^0 + 2v_{02}^0), \end{aligned}$$

$$\begin{aligned}
 \dot{q} &= -q^2 + p^2 - fp - 2r, \\
 \dot{p} &= -2pq + fq, \\
 \dot{r} &= -4qr - z_{10}^0(3u_{20}^0 + v_{11}^0) - z_{01}^0v_{20}^0 - \{z_0^0(3u_{30}^0 + v_{21}^0)\}, \\
 \dot{u}_{20}^0 &= -3qu_{20}^0 + p(u_{11}^0 - v_{20}^0) + fv_{20}^0 - \{3z_{30}^0\}, \\
 \dot{u}_{11}^0 &= -3qu_{11}^0 + p(2u_{02}^0 - 2u_{20}^0 - v_{11}^0) + fv_{11}^0 - \{2z_{21}^0\}, \\
 \dot{u}_{02}^0 &= -3qu_{02}^0 - p(u_{11}^0 + v_{02}^0) + fv_{02}^0 - \{z_{12}^0\}, \\
 \dot{v}_{20}^0 &= -3qv_{20}^0 + p(v_{11}^0 + u_{20}^0) - fu_{20}^0 - \{z_{21}^0\}, \\
 \dot{v}_{11}^0 &= -3qv_{11}^0 + p(2v_{02}^0 - 2v_{20}^0 + u_{11}^0) - fu_{11}^0 - \{2z_{12}^0\}, \\
 \dot{v}_{02}^0 &= -3qv_{02}^0 - p(v_{11}^0 - u_{02}^0) - fu_{02}^0 - \{3z_{03}^0\}.
 \end{aligned} \tag{6}$$

Here $V = (V_1, V_2)$ is the velocity of the singularity support $x = a(t)$, $q = u_{10}^0 = v_{01}^0$, $p = u_{01}^0 = -v_{10}^0$, $r = z_{20}^0 = z_{02}^0$, and $u_\alpha^0, v_\alpha^0, z_\alpha^0$ are coefficients of the expansion of the solution (2) in a neighborhood of the singularity support, i.e., $U^i = (u^i, v^i)$, $i = 0, 1$,

$$\begin{aligned}
 u^i &= \sum_{k=0}^{\infty} \sum_{|\alpha|=k} u_\alpha^i(t)(x - a(t))^\alpha, & v^i &= \sum_{k=0}^{\infty} \sum_{|\alpha|=k} v_\alpha^i(t)(x - a(t))^\alpha, \\
 z^i &= \sum_{k=0}^{\infty} \sum_{|\alpha|=k} z_\alpha^i(t)(x - a(t))^\alpha.
 \end{aligned}$$

The truncation of the sequence at the 14th term means that we neglect the terms in the braces in (6).

A comparison of numerical results with the actual track of the hurricane FORREST (21/09–31/09/1983, the Pacific Ocean) shows that there is a qualitative coincidence between these trajectories [8]. It was also shown that, besides (2), Eqs. (1) do not have any other singular solutions with pointwise support of the singularity [9] and that the truncated system (6) can be reduced to the Hill equation [10].

These results stimulated us to try to forecast the dynamics of hurricanes. It should be noted that we consider not simply a nonsmooth solution from a Banach space but a solution of some special structure and try to calculate the trajectory of motion its singularity. It is impossible to “catch” this solution by traditional methods for studying PDE. The authors developed a special method for estimating the error of the asymptotic with respect to smoothness solution. By using this method, the simplest version of the shallow water equations, i.e., the Hopf equation, has been studied [11]. Even in this special case, the estimation of the remainder turned out to be a very nontrivial problem. For the shallow water equations, this estimation must be more difficult. On the other hand, the obtained asymptotic solution could be compared with the results of the direct numerical computation for the shallow water equations. However, here we have a very complicated problem of setting the boundary conditions corresponding to the hurricane problem, which are necessary for numerical computations. Therefore, we decided to omit all stages that are traditional in the mathematical

study and to test the constructed asymptotic solution by using the forecasted hurricane motion.

We present the results of numerical calculations for three actually existing hurricanes (there we used the information about hurricane tracks delivered by the National Hurricane Center, USA). All results obtained can be judged as follows: the present approach is reasonable and competent and allows us to obtain a sufficiently good short-term forecast (not less than 24 hours). However, system (6) cannot be used for a long-term forecast. The results obtained allow us to assume that, most likely, this fact is related to defects of model (1) used here. Thus there is the problem of choosing an initial model that is more adequate than model (1), for which we need to construct a sequence of Hugoniot type equations and to carry out the corresponding numerical experiments.

This research was partially supported by the Russian Foundation for Basic Research, grants No. 99-01-01074 and No. 01-01-06057.

2 Numerical calculations of Hugoniot type equations. Long-term forecast

By truncating the system (6), we reduce the problem of calculating the dynamics of the hurricane center to the problem of solving a system consisting of 14 ordinary differential equations. There is the principal problem of choosing the Cauchy data. Our main idea is to choose the Cauchy data so that the trajectory calculated by the truncated system (6) be maximally close to a given track of an actual hurricane during some time interval $[0, t_{K+1}]$. Obviously, by studying the corresponding solution of (6) for $t > t_{K+1}$, we can forecast the further motion of the hurricane center.

Let us describe the algorithm that realizes this idea. By $\xi(t) = (\lambda(t), \varphi(t))$, $t \in [0, t_I]$, we denote the trajectory of an actual hurricane. Let $\xi_i = \xi(t_i)$ be the coordinates of the hurricane center at time $t_i = (i - 1)\Delta t$, where $i = 1, \dots, I$ is the measurement number and Δt is the time interval between successive measurements (usually, $\Delta t = 6$ hrs.). By $\mu^0 = (z_0^0|_{t=0}, \dots, v_{02}^0|_{t=0})$ we denote the set of initial data for system (6) and by $\mu(t_i, \mu^0)$ the solution of the Cauchy problem for (6) with the initial data μ^0 calculated at time t_i . Here and in the following, system (6) means that the system is truncated. We choose a number $K < I$ and carry out the following calculations.

1. Let us choose a point $\mu^0 \in \mathbb{R}^{14}$. We solve system (6) numerically using the Runge-Kutta method of order 4 and form the set $\{\mu(t_i, \mu^0) = (z_i^0(\mu^0), V_{1,i}(\mu^0), V_{2,i}(\mu^0), \dots)\}$, $i = 1, \dots, K + 1$.
2. We calculate the artificial trajectory of the hurricane: $\{\zeta_i(\mu^0) = (\bar{\lambda}_i, \bar{\varphi}_i)\}$, $i = 1, \dots, K + 1$, solving numerically the equations

$$\frac{d\bar{\lambda}}{dt} = V_1, \quad \frac{d\bar{\varphi}}{dt} = V_2, \quad \bar{\lambda}|_{t=0} = \lambda(0), \quad \bar{\varphi}|_{t=0} = \varphi(0). \quad (7)$$

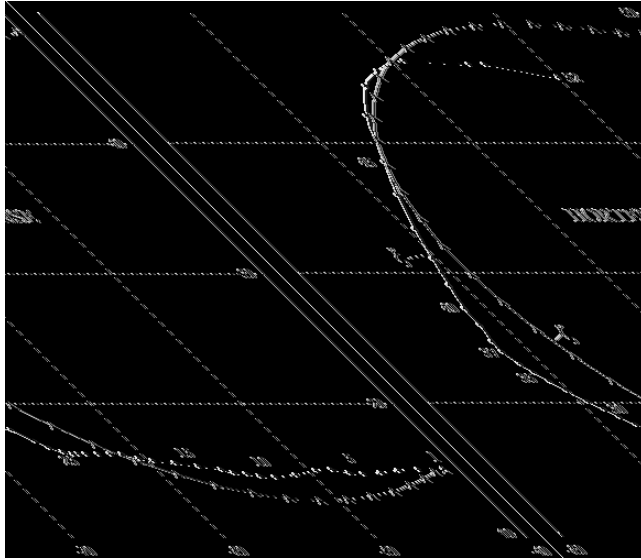


Figure 1: ξ is the track of HORTENSE starting at 12:00 a.m. 3/11 1996, ζ is the artificial trajectory. Initial data: $8.12 \cdot 10^{-5}$, -0.373 , 3.46 , 12.9 , 20.3 , 1 , $1.15 \cdot 10^{-3}$, $7.16 \cdot 10^{-11}$, $-8.22 \cdot 10^{-16}$, -10^{-16} , -10^{-16} , -10^{-16} , -10^{-16} , -10^{-16} . Distances: 0 , 0.99 , 1.40 , 1.61 , 1.71 , 2.04 , 2.72 , 3.11 , 3.00 , 3.07 , 3.85 , 5.03 , 6.16 , 7.53 , 8.18 , 8.98 , 9.94 , 11.4 , 12.8 , 14.6 , 16.5 , 18.5 , 20.6 , 22.7 , 24.6 , 26.3 , 27.7 , 28.7 .

3. We calculate the error function

$$J(K, \mu^0) = \sum_{i=1}^{K+1} |\xi_i - \zeta_i(\mu^0)|^2. \quad (8)$$

4. We find the value $\mu^0 = \mu_K^0$ at which $J(K, \mu^0)$ attains its minimum.

In numerical experiments we, first of all, verify the following hypothesis: if we increase the number K successively with the motion of the hurricane, then the trajectories $\zeta(t, \mu_K^0)$ obtained become closer and closer to the actual trajectory $\xi(t)$. In other words, the more hurricane prehistory we take into account, the better we forecast the motion of the hurricane. Obviously, this hypothesis assumes that there exist an initial point μ_I^0 such that the trajectories $\zeta(t, \mu_I^0)$ and $\xi(t)$ are close to each other on the entire time interval $[0, t_I]$.

For a test example, we considered the hurricane HORTENSE (03/09–16/09, 1996) and carried out numerous numerical experiments. The best result is shown in Fig. 1. Here and in subsequent figures the initial data are listed in the same order as the unknown functions in the left-hand side in (6), i.e., $z_0^0|_{t=t_1} = 8.12 \cdot 10^{-5}$, $V_1|_{t=t_1} = -0.373, \dots, v_{02}^0|_{t=t_1} = -1 \cdot 10^{-16}$. The unit of measurement of the distance on the spherical surface is 100 km.

One can readily see that, indeed, the artificial curve ζ is sufficiently close (from a qualitative geometrical viewpoint) to the actual trajectory ξ of the

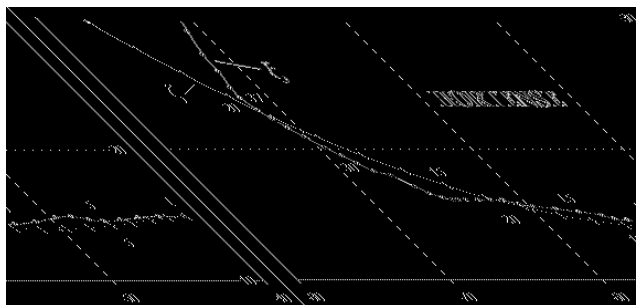


Figure 2: Initial data: $8.12 \cdot 10^{-5}$, -5.14 , 0.43 , $6.43 \cdot 10^{-3}$, 5.57 , 0.26 , 0.21 , $4.46 \cdot 10^{-10}$, -10^{-15} , -10^{-15} , -10^{-15} , -10^{-15} , -10^{-15} , -10^{-15} , -10^{-15} , $K=3$, $M=1$. Distances for approximation: 0 , 0.433 , 0.505 , 0.458 . Distances for forecast: 0.408 , 0.958 , 1.77 , 2.27 , 2.28 , 2.52 , 3.40 , 4.64 , 5.82 , 7.23 .

hurricane. Nevertheless, from the forecast viewpoint, the obtained “optimal” curve ζ is absolutely inconsistent, since, starting from the 14th node, the distances between $\xi(t_j)$ and $\zeta(t_j, \mu_I^0)$, $j \geq 14$, are greater than 750 km. This effect is caused by the fact that the velocity of the artificial hurricane is greater than the velocity of the actual hurricane HORTENSE. Due to this fact, the distance $|\xi(t_j) - \zeta(t_j, \mu_I^0)|$ increases with j . The dynamics of an increase in the error $|\xi(t_j) - \zeta(t_j, \mu_I^0)|$ for HORTENSE is shown in the comment to Fig. 1. Similar calculations for the hurricane GEORGES shown in Fig. 8 lead to the same result. Thus the above hypothesis is inconsistent and the probability of an appropriate long-term forecast is very small.

3 Short-term forecast

There is good reason to hope that a short-term forecast will be successful, since all calculations carried out according to the algorithm in Sec. 2 show that if $|\xi(t_{K+1}) - \zeta(t_{K+1}, \mu_K^0)|$ is small, then the distance between $\xi(t_{K+i})$ and $\zeta(t_{K+i}, \mu_K^0)$ for $i = 4 \div 8$ is comparable with the actual diameter of the hurricane eye ($i = 4 \div 8$ means the forecast for $24 \div 48$ hrs.).

To carry out a short-term dynamical forecast, we must slightly change the algorithm in Sec. 2. Namely, we choose a time instant t_M and write $\xi_M = (\lambda(t_M), \varphi(t_M))$ as the coordinates of the hurricane center for $t = t_M$. We choose the number K so that $K + M \leq I$ and perform the calculations similar to those in Sec. 2 but starting from $t = t_M$.

In contrast to the algorithm in Sec. 2, the main advantage is that $\zeta_M = \xi_M$ for all t_M . This means that we do not extremely accumulate the error arising in calculations of ζ_{M+K} . Moreover, we partly take into account the latitude variation of the Coriolis parameter by setting $f = 2 \sin \varphi(t_M)$ in our formulas.

Let us discuss the results of numerical experiments (Figs. 2–7) for the hurricane HORTENSE. In order to study the results obtained, we briefly consider the

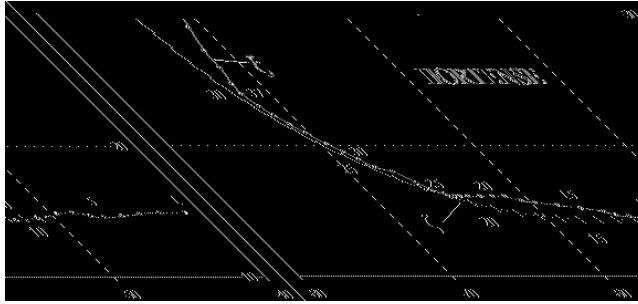


Figure 3: Initial data: $8.12 \cdot 10^{-5}$, -4.40 , 0.673 , $3.01 \cdot 10^{-3}$, 4.77 , 0.336 , $8.22 \cdot 10^{-2}$, $5.34 \cdot 10^{-10}$, -10^{-15} , -10^{-15} , -10^{-15} , -10^{-15} , -10^{-15} , -10^{-15} , -10^{-15} , $K=3$, $M=9$. Distances for approximation: 0 , 0.49 , 0.32 , 0.28 . Distances for forecast: 0.67 , 1.32 , 1.41 , 1.43 , 1.40 , 1.67 , 1.99 , 2.19 , 2.50 , 2.92 , 3.74 , 4.70 , 5.47 , 6.09 , 6.65 , 6.64 , 7.05 .

actual track. We conditionally divide the trajectory of the actual hurricane into three regions. In the first part that lasts from $t_1 = 0$ to $\approx t_{18} = 4.25 \sim 102$ hrs., the hurricane moves practically to the West over the ocean. In the second region (from $\approx t_{18}$ to $\approx t_{37} = 9 \sim 216$ hrs.), the hurricane changes the direction of motion from the West to the North–Northwest. In the vicinity of the 37th node, the hurricane makes a sharp turn to the Northeast. From the geographic viewpoint, for $t \approx t_{18}$, the hurricane comes to the Lesser Antilles Isles, moves over the Caribbean Sea towards the Haiti Isle, and then to the Bahamas. Another sharp turn is made approximately on the boundary between the Bahamas and the Atlantic Ocean. The third region of the hurricane trajectory (from $\approx t_{37}$ to $t_{52} = 13 \sim 306$ hrs.) is over the Atlantic Ocean. During approximately two days (from $\approx t_{37}$ to $\approx t_{47}$), the hurricane moves to the Northwest. Then it smoothly turns to the East. Of course, the boundaries of the regions are rather rough.

To the first region, there correspond results shown in Figs. 2, 3. We see that the artificial trajectory coincides well with the actual trajectory. Moreover, except for the velocity, the trajectories are astonishingly close to each other up to the turning point ξ_{37} . However the artificial and actual velocities are different, and thus only a short-term forecast can be reliable. So, for $t_M = 0$ (see Fig. 2), which corresponds to the forecast starting from $t_4 \sim 18$ hrs., the initial error is $|\Delta_4| \approx 46$ km (here and in the following, $\Delta_i = |\xi_i - \zeta_i|$ is the distance between ξ_i and ζ_i). The error increases to $\Delta_8 \approx 227$ km during the first 24 hrs. and to $\Delta_{12} \approx 464$ km during the next 24 hrs. For $M = 9$, $t_9 \sim 48$ hrs. (see Fig. 3), which corresponds to the forecast starting from $t_{12} \sim 66$ hrs., the initial error is $\Delta_{12} \approx 28$ km. The error increases to $\Delta_{16} \approx 140$ km during the first 24 hrs., to $\Delta_{20} \approx 220$ km during the next 24 hrs., and to $\Delta_{24} \approx 470$ km during the next 24 hrs.. If we take into account the fact that the maximum distance between the trajectories does not exceed 120 km till the node ξ_{37} , then the forecast is apparently successful.

Numerical results shown in Figs. 4, 5 correspond to the second part of the hurricane trajectory. We see that the approximating properties of the artificial

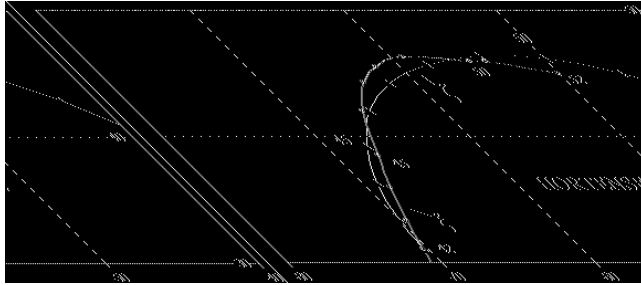


Figure 6: Initial data: $8.12 \cdot 10^{-5}$, 0.449, 1.09, 8.51, 40.3, 1.21, $5.63 \cdot 10^{-3}$, $6.64 \cdot 10^{-11}$, -8.2210^{-16} , -10^{-16} , -10^{-16} , -10^{-16} , -10^{-16} , -10^{-16} , -10^{-16} , $K=3$, $M=42$. Distances for approximation: 0, 0.44, 0.69, 0.84. Distances for forecast: 0.26, 1.22, 2.65, 3.84, 3.88, 6.37.

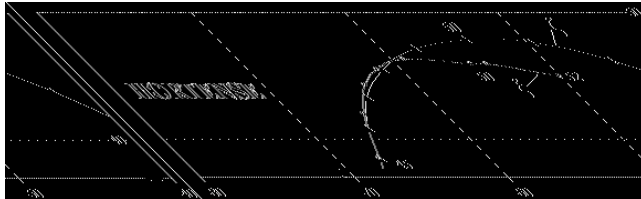


Figure 7: Initial data: $8.12 \cdot 10^{-5}$, 1.38, 3.36, 1.29, 30.4, 0.913, $1.16 \cdot 10^{-2}$, $7.95 \cdot 10^{-11}$, -8.2210^{-16} , -10^{-16} , -10^{-16} , -10^{-16} , -10^{-16} , -10^{-16} , -10^{-16} , $K=3$, $M=45$. Distances for approximation: 0, 1.46, 1.22, 0.23. Distances for forecast: 1.40, 2.28, 3.71, 3.60.

latitudes ($\approx 15^\circ$) almost parallel to the equator, and the external factors seem to be constant. In numerical calculations according to the truncated sequence of Hugoniot type conditions (6), the artificial and actual trajectory practically coincide (see Figs. 1–3) and the velocity is sufficiently close to the actual velocity of the hurricane. These results prove that the representation of the solution in the form of the expansion with respect to smoothness (2) possesses good approximating properties and it is possible to use the truncated Hugoniot sequence (6) for calculating actual hurricane tracks.

The second part of the hurricane trajectory goes over the Caribbean Sea. There is an increasing deviation to the North in the actual trajectory, and the hurricane velocity decreases. Apparently, this is due to a change in the water temperature. The trajectory of the artificial hurricane calculated according to the initial data corresponding to the first region (Figs. 2 and 3) is close to the actual trajectory. However, the velocity of the artificial hurricane does not decrease. If the initial data are chosen according to the measurements in the second region (Fig. 4), then the velocity of the artificial hurricane turns out to be close to the velocity of the actual hurricane (in the second region). However, the approximating properties of the numerical trajectory become worse as the hurricane moves to the North. Apparently, this is due to the fact that model (1) becomes less adequate. It was assumed that φ is “constant” and small, while

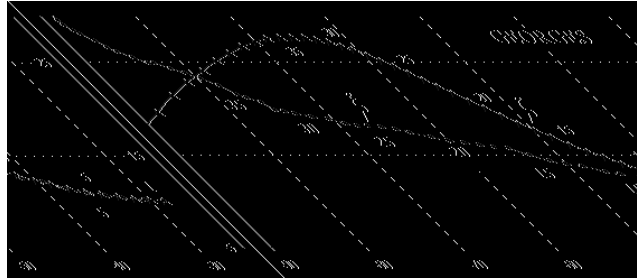


Figure 8: ξ is the track of GEORGES starting at 03:00 a.m. 16/09 1998, ζ is the artificial trajectory. Initial data: $8.12 \cdot 10^{-5}$, -5.99 , $4.06 \cdot 10^{-2}$, $1.33 \cdot 10^{-8}$, 1.32 , $5.04 \cdot 10^{-2}$, $7.52 \cdot 10^{-2}$, $6.98 \cdot 10^{-12}$, -2.0810^{-14} , -1.8910^{-14} , -1.7210^{-14} , -1.9110^{-14} , -1.7410^{-14} , -1.7410^{-14} . Distances: 0, 0.45, 1.13, 1.26, 1.64, 1.93, 2.34, 2.82, 3.42, 4.22, 4.33, 4.99, 5.31, 5.46, 5.83, 6.33, 6.84, 7.27, 7.90, 8.60, 9.32, 10.2, 10.7.

the coordinates of the actual hurricane vary by $\approx 10^\circ$ in the latitude.

Over the boundary between the Bahamas and the Atlantic Ocean, the actual hurricane passes from the second part of the trajectory to the third part. This passage is accompanied by a sharp change in the direction of motion and an increase in the velocity. Apparently, the difference between the water temperature in the Bahamas region and in the Atlantic Ocean (at latitudes higher than $\approx 25^\circ$) is a decisive factor here. The artificial hurricane calculated according to the initial data measured in the second region (Fig. 5) moves significantly lower than the actual hurricane (as if the hurricane still remained in the second region), and its trajectory is qualitatively close to the actual trajectory only on a comparatively small region. By choosing the initial data so that they correspond to the conditions in the third region (Figs. 6, 7), we obtain a closer correspondence between the velocities of the actual and artificial hurricanes. In this case we have a qualitative coincidence between the trajectories on a larger region.

4 Other examples

The test example of the hurricane HORTENSE is a typical example. Namely, most of the hurricanes actually existing in the Atlantic Ocean have similar trajectories. Now we consider two hurricanes, which are exceptional in some sense.

The trajectory of the hurricane GEORGES (15/09–28/09/1998) almost completely lies in the tropical belt and is practically in a straight line to the West–Northwest. We *a priori* believe that the forecast of its dynamics will be successful.

The trajectory of the hurricane NICOLE (24/11–01/12/1998) lies further north in the Atlantic Ocean, makes a sufficiently sharp turn (through $\approx 130^\circ$), and has a bend towards the West. We *a priori* expect that the quality of the

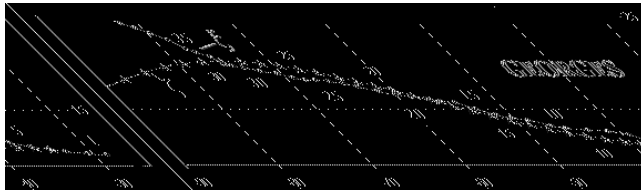


Figure 9: Initial data: $8.12 \cdot 10^{-5}$, -6.86 , 0.155 , $2.04 \cdot 10^{-9}$, 1.84 , $2.58 \cdot 10^{-2}$, $8.62 \cdot 10^{-2}$, $1.46 \cdot 10^{-11}$, -1.2910^{-14} , -1.2910^{-14} , -1.2910^{-14} , -1.4310^{-14} , -1.3010^{-14} , -1.3010^{-14} , $K=15$, $M=4$. Distances for approximation: 0, 0.24, 0.50, 1.16, 1.26, 1.53, 1.21, 1.57, 1.38, 1.08, 1.10, 1.27, 0.81, 0.44, 0.26. Distances for forecast: 0.54, 0.67, 0.73, 0.92, 1.18, 1.64, 2.31, 2.86, 3.24, 3.50, 4.09, 5.48, 7.11, 9.43, 11.7, 14.5.

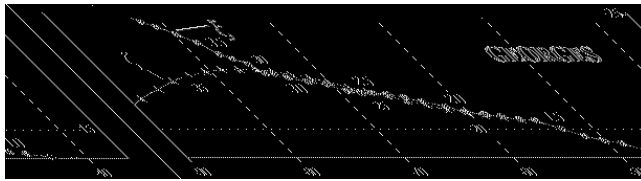


Figure 10: Initial data: $8.12 \cdot 10^{-5}$, -6.12 , 0.113 , $1.82 \cdot 10^{-9}$, 2.45 , $2.30 \cdot 10^{-2}$, $9.38 \cdot 10^{-2}$, $1.59 \cdot 10^{-11}$, -1.2910^{-14} , -1.2910^{-14} , -1.2910^{-14} , -1.4310^{-14} , -1.3010^{-14} , -1.3010^{-14} , $K=9$, $M=16$. Distances for approximation: 0, 0.13, 0.38, 0.46, 0.53, 0.50, 0.38, 0.48, 0.53, 0.62. Distances for forecast: 1.07, 1.41, 1.46, 1.26, 1.17, 1.70, 2.31, 3.33, 4.22, 5.50, 6.42, 8.93.

forecast of its dynamics will be bad.

1. The hurricane GEORGES was first observed on 15/09/1998 in the far eastern Atlantic. Moving practically in a straight line on a general West–Northwest course, the hurricane entered the Lesser Antilles Isles in 5 days and passed over practically all the Greater Antilles Isles. Then, still moving practically in a straight line, the hurricane crossed the Gulf of Mexico and decayed to the North of New Orleans. The fact that the hurricane did not make sharp turns can be treated as “stability” of external factors.

The plot in Fig. 8 shows the results (similar to those in Fig. 1) obtained in calculating the artificial trajectory that is maximally close to the entire actual trajectory of the hurricane. We see that the difference between the trajectories exceeds 850 km on the middle part and, on the final stage, the artificial hurricane moves to the South–West, whereas the actual hurricane moves to the North–West and the difference between the trajectories exceeds 1000 km. If we take into account the velocity of the hurricane, then the difference between the actual and artificial hurricanes is more significant for large t . This result confirms the conclusion drawn in Sec. 2 that system (6) does not work well for long-term forecasts.

Let us discuss the results of the short-term forecast. Approximately at t_{32} GEORGES made landfall in the Cuba isles. Undoubtedly, this was the reason for

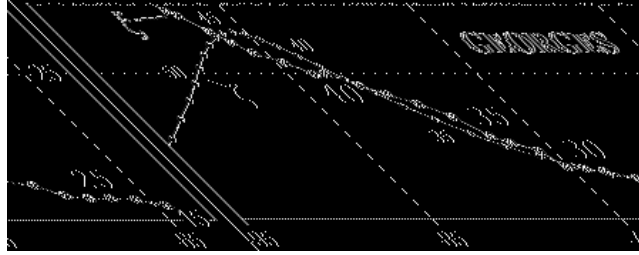


Figure 11: Initial data: $8.12 \cdot 10^{-5}$, -6.18 , 0.171 , $1.84 \cdot 10^{-9}$, 2.03 , $2.33 \cdot 10^{-2}$, $7.75 \cdot 10^{-2}$, $1.60 \cdot 10^{-11}$, -1.2910^{-14} , -1.2910^{-14} , -1.2910^{-14} , -1.4310^{-14} , -1.3010^{-14} , -1.3010^{-14} , $K=6$, $M=28$. Distances for approximation: 0, 0.12, 0.15, 0.54, 1.17, 1.73, 1.95. Distances for forecast: 2.35, 2.26, 2.02, 1.80, 1.68, 1.34, 1.85, 1.53, 1.23, 0.87, 0.54, 1.45, 2.08, 3.34, 4.74, 6.60, 8.26, 10.1.

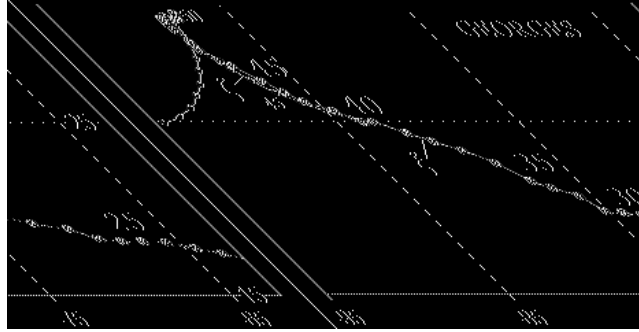


Figure 12: Initial data: $8.12 \cdot 10^{-5}$, -4.50 , 0.227 , $1.34 \cdot 10^{-9}$, 1.48 , $2.07 \cdot 10^{-2}$, $5.65 \cdot 10^{-2}$, -1.2910^{-14} , -1.2910^{-14} , -1.2910^{-14} , -1.4310^{-14} , -1.3010^{-14} , -1.3010^{-14} , $K=6$, $M=40$. Distances for approximation: 0, 0.56, 0.48, 0.29, 0.50, 0.57, 0.33. Distances for forecast: 0.45, 0.39, 0.50, 0.24, 0.33, 0.72, 0.49, 0.66.

a slight change in his trajectory. The artificial hurricane based on the hurricane prehistory cannot predict this turning point. Moreover, it predicts a smooth turn to the South. Correspondingly, we can see in Figs. 9, 10 that the long-term forecasts are qualitatively wrong. However, all these forecasts are good for ≈ 60 hrs.

The last group of plots (see Figs. 11, 12) corresponds to the forecast for $t \geq t_{34}$. This means that by choosing $\mu_{K,M}^0$ we take into account the turns made by GEORGES at $t = t_{32}$ and $t = t_{33}$. We see that the forecast quality sharply increases in contrast to Figs. 9, 10. Moreover, we see that the forecast quality increases with t_{K+M} and is practically ideal for $t > t_{46}$ (see Fig. 12). Curiously enough, all these forecasts show that the hurricane makes a turn at a longitude of 27° – 33° , although the beach was not taken into account in model (1).

So, we see that our *a priori* assumption that model (1) and system (6) are

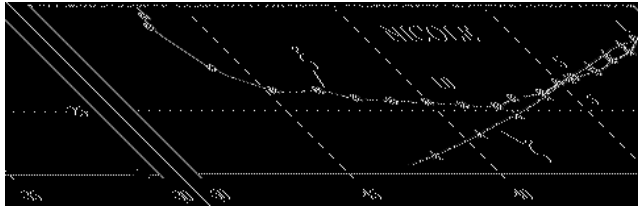


Figure 13: ξ is the track of NICOLE starting at 09:00 a.m. 25/11 1998, ζ is the artificial trajectory. Initial data: $8.12 \cdot 10^{-5}$, -2.64 , $1.33 \cdot 10^{-2}$, 0.10 , 4.75 , $2.22 \cdot 10^{-2}$, 0.165 , $4.22 \cdot 10^{-9}$, -9.810^{-16} , -9.810^{-16} , -9.810^{-16} , -9.810^{-16} , -9.810^{-16} , -9.810^{-16} , $K=3$, $M=1$. Distances for approximation: 0, 0.35, 0.31, 0.28. Distances for forecast: 0.32, 1.08, 1.82, 2.77, 4.26, 6.02, 8.19, 10.8, 13.9.

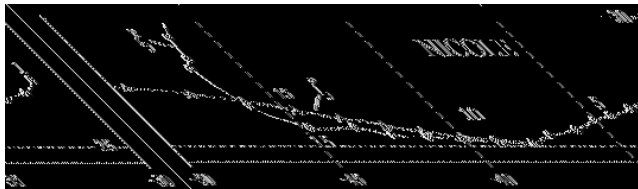


Figure 14: Initial data: $8.12 \cdot 10^{-5}$, -4.21 , $9.50 \cdot 10^{-3}$, 0.195 , 2.77 , $3.54 \cdot 10^{-2}$, 0.321 , $4.22 \cdot 10^{-9}$, -9.810^{-16} , -9.810^{-16} , -9.810^{-16} , -9.810^{-16} , -9.810^{-16} , -9.810^{-16} , -9.810^{-16} , $K=3$, $M=9$. Distances for approximation: 0, 0.03, 0.09, 0.22. Distances for forecast: 0.41, 0.45, 0.75, 0.23, 1.44, 3.26, 5.86, 10.0, 16.3.

sufficiently adequate for forecasting the hurricane GEORGES is true.

2. The behavior of the hurricane NICOLE was affected by powerful external factors. This hurricane, first observed on 24/11/1998 about 700 miles to the West of the Canary Isles, initially moved to the South–West and then turned to the West. About 96 hrs. later, the hurricane sharply changed the direction of its motion and moved to the Northeast. Next, about 30 hrs. after the turn, the trajectory of the hurricane started to bend in the direction opposite to the action of the Coriolis force.

Because of such behavior of NICOLE, one can hardly expect that model (1) can describe the actual trajectory. Nevertheless, the numerical experiments performed show that our algorithms provide a sufficiently good forecast for 24 hrs.

Figure 13 shows the artificial trajectory calculated for $K = 3$ and $M = 1$, which corresponds to the forecast for $t > t_4 = 18$ hrs. We see that the artificial and actual trajectories agree sufficiently well until the turning point of the actual hurricane.

The calculations of the next sloping part of the trajectory ($K = 3$, $M = 9$, see Fig. 14) yield extremely good qualitative forecast for 24 hrs. ($\Delta_{16} \approx 23$ km). Nevertheless, the artificial hurricane still does not forecast the turn of the trajectory, and therefore, the error of the forecast for the second 24 hrs.

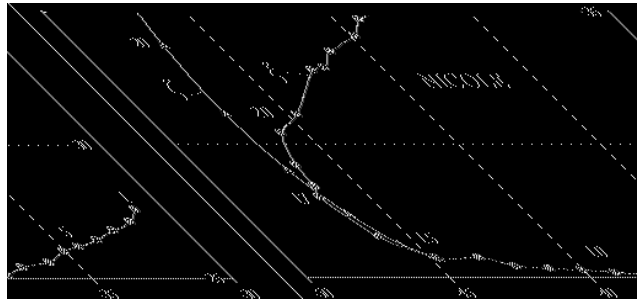


Figure 15: Initial data: $8.12 \cdot 10^{-5}$, -2.15 , -1.56 , 4.47 , -8.10 , 0.233 , 0.299 , $4.84 \cdot 10^{-11}$, -8.2210^{-16} , -10^{-16} , -10^{-16} , -10^{-16} , -10^{-16} , -10^{-16} , -10^{-16} , $K=3$, $M=15$. Distances for approximation: 0 , 0.56 , 0.79 , 0.84 . Distances for forecast: 2.37 , 3.91 , 6.30 , 7.84 , 10.9 , 13.7 .

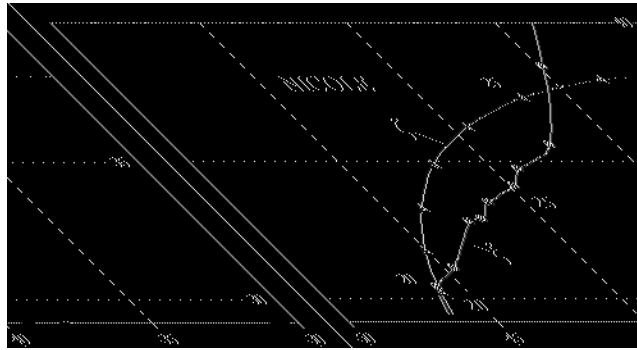


Figure 16: Initial data: $8.12 \cdot 10^{-5}$, -6.6310^{-3} , -0.891 , 0.126 , -12.6 , 0.363 , 0.255 , $4.84 \cdot 10^{-11}$, -8.2210^{-16} , -10^{-16} , -10^{-16} , -10^{-16} , -10^{-16} , -10^{-16} , -10^{-16} , -10^{-16} , $K=3$, $M=18$. Distances for approximation: 0 , 0.09 , 0.13 , 0.83 . Distances for forecast: 1.24 , 2.19 , 3.43 , 4.57 , 6.32 , 7.28 .

increases to $\Delta_{19} \approx 590$ km, while $\Delta_{20} \approx 1000$ km.

One can hardly say that the forecast is successful in the region containing the turning point of NICOLE (see Fig. 15). The initial error is $\Delta_{18} \approx 84$ km for t_{18} , then it increases approximately by 200 km every 6 hrs., so that we obtain $\Delta_{22} \approx 780$ km after 24 hrs. This failure can easily be explained, since the forecast shown in Fig. 15 is based on the hurricane trajectory till the turn at t_{17} .

After the hurricane changes the direction of its motion, the forecast quality improves to some extent. Here a decisive factor is the fact that we forecast the motion of NICOLE on the basis of its trajectory after the turning point. The plot in Fig. 16 ($K = 3$, $M = 18$) shows that the trajectories are qualitatively close to one another until the latitude $\approx 37^\circ$ is achieved. Next, under the action of the Coriolis force, the artificial hurricane continues to move to the East, while the actual hurricane moves to the Northeast. An attempt to improve the

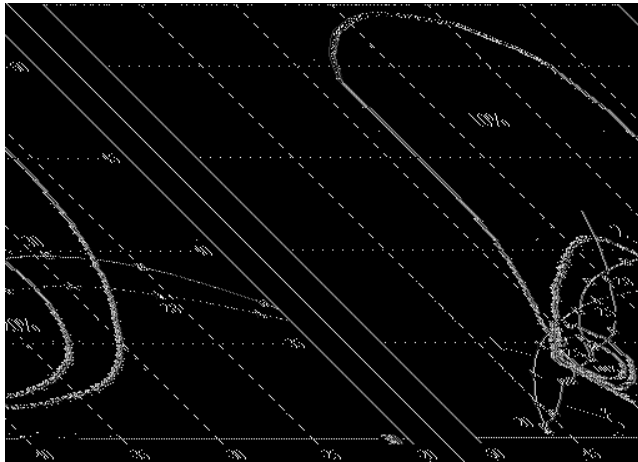


Figure 17: Probability that center of NICOLE will pass within 75 miles during the 72 hours starting at 10:00 a.m. 30/11 1998 (the National Hurricane Center, USA) Contour levels shown are 10%, 20% 50%, and 100%. ξ is the track of NICOLE, curve 1 is the solution of (6) for $K=3$ and $M=18$, curve 2 is the solution of (6) for $K=3$ and $M=25$.

situation by using a longer prehistory made the forecast quality even worse. Similar pictures are observed for the forecasts starting from t_{24} and from t_{28} : the actual and artificial hurricanes still behave in qualitatively different ways.

5 Conclusions

The analysis of numerical results shows that, on all parts of the hurricane track corresponding to more or less stable external factors, the artificial trajectories calculated by the truncated system (6) (with the initial data corresponding to this particular part) qualitatively and quantitatively coincide to a satisfactory extent with the actual trajectories. This coincidence is rather close in the low latitudes and becomes worse as the hurricane moves to the North. Both facts correspond to an *a priori* analysis of whether model (1) is adequate.

Therefore, we can draw the conclusion that the truncated system (6) possesses sufficiently good approximating properties. This conclusion holds for a time interval of several days. However, to use the truncated system (6) on larger time intervals is rather problematic. The plots in Figs. 4, 5 clearly demonstrate that there are restrictions on the long term applicability of this system. The trajectory “breakdown” (after the calculation time ≈ 150 hrs.) is closely related to an increase in the error arising due to the truncation of the infinite system of equations. Similar “breakdowns” can be seen in other figures, however, they occur at a considerable distance from the trajectory of the actual hurricane. Thus the error due to the truncation manifests itself after sufficiently large time and is unessential for short-term and medium-term forecast. Next, numerical

results obtained do not allow us to hope that a good forecast can be obtained by using (6) in the case of a sharp change in the trajectory. The hurricane NICOLE gives the most illustrative example of this fact. There is no doubt that this fact is closely related to the defects of the initial model (1).

In order to estimate the results of numerical experiments, let us compare the artificial trajectory of NICOLE with the probability forecast made by the National Hurricane Center at 10:00 a.m. 30/11/1998. This forecast was made almost at the same time as our forecast shown in Fig. 16, since the choice $K = 3$, $M = 18$ implies the absolute time $t_{21} = 09:00$ a.m. 30/11/1998. The comparison of the probability forecast with the actual NICOLE trajectory for $t > t_{21}$ (see Fig. 17) shows that during 36 hrs. the actual hurricane approaches the 20% region and then, after 3 days, enters the 10% region. This means that the predicted probability $p = 0.8$ (that the eye of NICOLE stays in the 20% region during 72 hrs.) is too excessive. Only the probability $p = 0.9$ (that NICOLE stays in a considerably larger 10% region) is adequate. The forecast obtained by using system (6) (for $K = 3$, $M = 18$, curve 1 in Fig. 17) predicts that the trajectory leaves the 20% region during 36 hrs. In this sense our forecast is even better than the professional forecast. However, as shown above, the artificial trajectory qualitatively differs from the actual trajectory. We can partially improve this forecast by using the dynamical correction (curve 2 in Fig. 17). Thus, although the basic model (1) is rough, the quality of our forecast is comparable (even if somewhat worse) with the quality of the professional forecast.

All numerical experiments resulted in a sufficiently good forecast for 24–48 hrs. Apparently, the forecast of extremely high quality in Fig. 4 (more than for 5 days) is accidental. Nevertheless, several successful medium-term forecasts, including the 3-day forecasts (Figs. 3, 11) make us optimistic.

Finally, the results obtained show that the following fundamental hypotheses hold:

- Methods of the theory of generalized functions can be used for calculating the dynamics of a hurricane;
- A hurricane can be treated as a weak pointwise singularity;
- The singularity dynamics can be calculated by using a truncated sequence of Hugoniot type conditions.

It is highly probable that we can improve the quality of short-term and medium-term forecasts by choosing a basic model that is more adequate than model (1).

References

- [1] E. E. Gossard and W. H. Hooke, *Waves in the Atmosphere*, Elsevier, Amsterdam, 1975.
- [2] E. Lorenz, *Nature and Theory of General Circulation in the Atmosphere* [Russian Translation], Gidrometeoizdat, Leningrad, 1971.

- [3] A. M. Obukhov, *On the geostrophic wind problem*, Izv. Akad. Nauk SSSR, Ser. Geogr, **13**:4 (1949), 281–306.
- [4] J. Pedlosky, *Geophysical Fluid Dynamics*, Springer, Berlin, 1982.
- [5] J.-L. Lions, R. Temam, and S. Wang, *New formulations of the primitive equations of atmosphere and applications*, Nonlinearity, **5** (1992), 237–288.
- [6] V. P. Maslov, *Three algebras corresponding to nonsmooth solutions of systems with quasilinear hyperbolic equations*, Russ. Math. Surv., **35**:2 (1980), 252–253.
- [7] V. N. Zhikharev, *Necessary conditions for the existence and the type uniqueness of a solution with weak pointwise singularity to two-dimensional equations of hydrodynamics*, Dep. VINITI No. 8148-B86, Moscow, 1986.
- [8] V. V. Bulatov, Yu. V. Vladimirov, V. G. Danilov, and S. Yu. Dobrokhotov, *Propagation of a pointwise algebraic singularity for two-dimensional nonlinear equations of hydrodynamics*, Mat. Zametki, **55**:3 (1994), 11–20 (in Russian); English translation in Math. Notes.
- [9] S. Yu. Dobrokhotov, K. V. Pankrashkin, and E. S. Semenov, *Proof of Maslov's conjecture about the structure of weak point singular solution of the shallow water equations*, Russian J. of Math. Physics, **8**:1, 2001, 25–52.
- [10] S. Yu. Dobrokhotov, *Hugoniot–Maslov chain for solitary vortices of the shallow water equations. I. Derivation of the chains for the case of variable Coriolis forces and reduction to the Hill equation*, Russ. J. of Math. Phys., **6**:2 (1999).
- [11] V. G. Danilov and G. A. Omel'yanov, *Calculation of the singularity dynamics for quadratic nonlinear hyperbolic equations. Example: the Hopf equation*, Nonlinear Theory of Generalized Functions (Vienna, 1997, M.Grosser et al., eds.), Res. Notes in Math., vol.401, Chapman and Hall, London, 1999, 63–74.

VLADIMIR DANILOV (e-mail: pm@miem.edu.ru)

GEORGII OMEL'YANOV

DANIIL ROZENKNOP

Moscow State Institute of Electronics and Mathematics,

B. Trekhsvyatitel'skii per., 3/12,

Moscow 109028, Russia